Insect Biochemistry and Molecular Biology 113 (2019) 103215

Contents lists available at ScienceDirect

Insect Biochemistry and Molecular Biology

journal homepage: www.elsevier.com/locate/ibmb

Identification of novel antimicrobial peptides from rice planthopper, *Nilaparvata lugens*

Xiang Zhou[a], Lu-Yao Peng[a], Zhe-Chao Wang[a], Wei Wang[a], Zhen Zhu[a], Xiao-Hui Huang[a], Li-Bo Chen[a], Qi-Sheng Song[b,**], Yan-Yuan Bao[a,*]

[a] State Key Laboratory of Rice Biology and Ministry of Agriculture Key Lab of Molecular Biology of Crop Pathogens and Insect Pests, Institute of Insect Sciences, Zhejiang University, Hangzhou, 310058, China
[b] Division of Plant Sciences, College of Agriculture, Food and Natural Resources, University of Missouri, USA

ARTICLE INFO

Keywords:
Nilaparvata lugens
Lugensin
PGRP-LC
Antibacterial activity

ABSTRACT

In this study, two novel antibacterial peptide genes, termed *lugensin* A and B were identified and characterized from a rice sap-sucking hemipteran insect pest, the brown planthopper, *Nilaparvata lugens*. *Lugensin* gene expression was significantly induced by Gram-negative and Gram-positive bacterial stains under the regulation of a signal receptor, the long peptidoglycan recognition protein (PGRP-LC) in the IMD pathway. Knockdown of *PGRP-LC* by RNAi eliminated bacterium induced Lugensin gene expression. Lugensins had the apparent antibacterial activities against *Escherichia coli* K12, *Bacillus subtilis* and the rice bacterial brown stripe pathogen *Acidovorax avenae* subsp. *avenae* (*Aaa*) strain RS-1. Lugensins inhibited bacterial proliferation by disrupting the integrity of the bacterial membranes. Scanning electron microscopy revealed abnormal membrane morphology of the recombinant Lugensin-treated bacteria. Lugensins induced complete cell disruption of *E. coli* K12 and *B. subtilis* strains while formed the holes on the cell surface of *Aaa* RS-1 strain. Immunofluorescence showed that Lugensins localized in the cell membrane of *E. coli* K12 while accumulated in the cytosol of *B. subtilis*. Differently, Lugensins remained in both the cell membrane and the cytosol of *Aaa* RS-1 strain, suggesting different action modes of Lugensins to different microbes. This is the first report of the novel antibacterial peptides found in the rice sap-sucking hemipteran insect species.

1. Introduction

Insects rely on innate immune system to fight off pathogenic microorganisms. Antimicrobial peptides are the potent native defense molecules combating foreign pathogens, *i.e.*, bacteria and fungi. So far, 295 antimicrobial peptides have been identified in a variety of insect species according to the Antimicrobial Peptide Database (http://aps.unmc.edu/AP/) (Wang et al., 2015). Based on amino acid composition and structural motif feature, insect antimicrobial peptides can be divided into four classes: α-helical peptides (cecropin and moricin), cysteine-rich peptides (insect defensin and drosomycin), proline-rich peptides (apidaecin, drosocin, and lebocin) and glycine-rich peptides (attacin and gloverin) (Yi et al., 2014). Some antimicrobial peptides like moricin and gloverin have been found only in Lepidoptera while metchnikowin is restricted to *Drosophila* (Gerardo et al., 2010). Antimicrobial peptide gene expression was mainly regulated by the Toll and immune deficiency (IMD) signaling pathways, which are highly conserved in flies (*Drosophila* spp.), mosquitos (*Aedes aegypti*, *Anopheles gambiae*), bees (*Apis mellifera*), worms (*Bombyx mori*) and beetles (*Tribolium castaneum*)(Christophides et al., 2002; Evans et al., 2006; Hetru and Hoffmann, 2009; Lemaitre and Hoffmann, 2007; Sackton et al., 2007; Tanaka and Yamakawa, 2011; Waterhouse et al., 2007). The phloem-sap-feeding hemipteran species, however, have significantly reduced number of immune-related molecules critical for recognition, signaling and killing of pathogens in insect defense system. For example, the pea aphid *Acyrthosiphon pisum* are missing many of the antimicrobial peptide genes, *i.e.*, *defensins* and *cecropins* common to other insects (Eisen, 2010; Gerardo et al., 2010; Laughton et al., 2011). The whitefly *Bemisia tabaci* has few antimicrobial peptides. Only *defensin*, *knottin* and *thaumatin* have been identified in *B. tabaci* genome thus far (Chen et al., 2016; Mahadav et al., 2008). Phloem-sap-feeding hemipteran insects appear to have a limited innate immune system compared to the other genome-sequenced insects.

The brown planthopper, *Nilaparvata lugens* (Hemiptera:

* Corresponding author.
** Corresponding author.
E-mail addresses: songq@missouri.edu (Q.-S. Song), yybao@zju.edu.cn (Y.-Y. Bao).

https://doi.org/10.1016/j.ibmb.2019.103215
Received 25 June 2019; Received in revised form 14 August 2019; Accepted 18 August 2019
Available online 23 August 2019
0965-1748/

Delphacidae), the most destructive rice pest, is a typical monophagous herbivore that exclusively depends on rice sap for survival. *N. lugens* faces a variety of environmental challenges including pathogenic infection. The nature of innate immunity in this phloem sap-feeding insect has not been understood yet. Having the annotated genome and transcriptome data enabled us to investigate immune responsive effector genes in *N. lugens*. However, we were only able to identify two immune effectors, defensin A and B, in *N. lugens* using bioinformatics approach (Bao et al., 2013). Species-specific immune effectors may present in *N. lugens* but remain undiscovered. To better understand the immune defense mechanism in *N. lugens*, in this study, we attempted to identify the immune-inducible defense molecules and characterized their regulation and action mechanisms.

Among the genome-available plant sap-sucking hemipteran insects, *A. pisum* and *B. tabaci* seem to be losing *PGRP-LC*, *IMD*, *dFADD*, *Dredd* and *Relish* genes crucial for the IMD immune pathway (Chen et al., 2016; International Aphid Genomics Consortium, 2010), thus they may fail to produce the immune effectors regulated by this signaling pathway. In contrast, the orthologous genes in the IMD pathway were well conserved in *N. lugens* (Bao et al., 2013), suggesting an intact immune response pathway in this insect species. This study set out to target the IMD pathway to find the immune responsive effectors. PGRP-LC was known as a key signal receptor in the IMD pathway to response primarily Gram-negative bacteria and some Gram-positive bacteria, and mediate the inducible synthesis of antibacterial peptides (Dziarski, 2004; Hultmark, 2003). In our previous study, we identified and cloned a *PGRP-LC* gene based on the *N. lugens* genome and transcriptome database (Bao et al., 2013). A transmembrane region was present in PGRP-LC sequence, suggesting that it may act as a cell surface receptor. In this present study, we initiated to investigate the immune effector genes by inhibiting *PGRP-LC* expression using RNA interference (RNAi) combined with RNA-Seq transcriptome sequencing. *N. lugens* is susceptible to RNAi, thus it is a good insect model system to study molecular functions of targeted genes. High efficiency of RNAi knockdown of functional genes has been achieved in this insect species (Huang et al., 2015, 2016; Wang et al., 2012; Wu et al., 2012; Xi et al., 2014, 2015a, 2015b; Xu et al., 2013, 2015, 2017; Zhang et al., 2015). In this study, we identified and characterized two *PGRP-LC* controlled genes. They shared 76.8% sequence identities at the deduced amino acid levels. Their sequences do not contain any characteristic domains and have no significant homologies with known immune molecules. We designated them as *lugensin* A and B as they had not yet been reported in any other insect species. Gram-positive bacterium *B. subtilis* and Gram-negative bacteria *E. coli* K12 significantly induced *lugensin* gene expression in *N. lugens* nymphs. The Gram-negative bacterium *Aaa* strain RS-1, a seed-borne pathogen causing bacterial brown stripe of rice, had much strong activity to trigger *lugensin* gene expression than *E. coli* K12 and *B. subtilis* bacteria. The recombinant Lugensin proteins showed apparent bactericidal activities toward above bacteria by disrupting the cell membranes. Bioinformatics analysis and experimental evidences clearly indicate that Lugensins are novel insect antibacterial peptides.

2. Materials and methods

2.1. Insects and bacteria

The *N. lugens* populations were originally collected from a rice field in the Huajiachi Campus of Zhejiang University, Hangzhou, China, in 2008. The insects were reared at 26 ± 0.5 °C with 50 ± 5% humidity on rice seedlings (*Oryza sativa* strain Xiushui 134) under a 16:8 h light: dark photoperiod as previously described (Huang et al., 2016).

Bacteria *Escherichia coli* K12 and *Bacillus subtilis* strains were routinely maintained in our lab on Luria-Bertani (LB) agar/broth (0.5% yeast extract, 1% peptone, 1% NaCl and 1.5% agar, pH 7.0) at 37 °C. Rice bacterial brown stripe pathogen *Acidovorax avenae* subsp. *avenae* (*Aaa*) strain RS-1 originally isolated from diseased rice in Zhejiang Province of China was kindly provided by Prof. Bin Li, Department of Applied Bioscience of Zhejiang University. The *Aaa* strain RS-1 was refreshed and grown on LB medium at 30 °C as described (Zhang et al., 2017).

2.2. Identification of PGRP-LC regulated immune effectors using RNA interference (RNAi) and high-throughput RNA-seq

A 508 bp of *PGRP-LC* sequence was cloned into the pMD19-T vector (TaKaRa, Dalian, China). Double-stranded RNAs were synthesized by *in vitro* transcription with PCR-generated DNA templates using the T7 RNAi Transcription Kit-BOX 1 (Vazyme, Nanjing, China). *Aequorea victoria* green fluorescent protein (GFP) gene was used as a control. Following transcription, the DNA template was removed with DNase (Vazyme, Nanjing, China). The size of dsRNA products was confirmed by electrophoresis on a 1% agarose gel with TAE buffer. The *PGRP-LC* and *GFP* primers used to generate the DNA template are shown in Table S1. Each fifth-instar *N. lugens* nymph was anaesthetized with carbon dioxide and microinjected with approximately 250 ng of ds*PGRP-LC* or ds*GFP* using the FemtoJet Microinjection System (Eppendorf-Netheler-Hinz, Hamburg, Germany). The nymphs were injected with a mixed heat-killed *E. coli* K12 and *B. subtilis* 24 h following RNAi. The treated insects were reared on rice seedlings at 26 ± 0.5°Cwith 50 ± 5% relative humidity under a 16:8 h light: dark photoperiod. Fat bodies were isolated from dsRNA-treated and bacteria-immunized nymphs 24 h later. Total RNA was extracted from the fat bodies and subjected to RNA-seq analysis. Differentially expressed sequences were compared among ds*GFP* treated, bacteria challenged, ds*PGRP-LC* treated, and bacteria challenged groups. The sequences were identified against the *N. lugens* genomic and transcriptomic databases as previously described. The differentially expressed genes were validated by aligning to the non-redundant (nr) National Center for Biotechnology Information (NCBI) nucleotide database using a cut-off E-value of 10^{-10}. The exon–intron organizations of genes were predicted based on the mRNA-genome alignments at the NCBI Splign (https://www.ncbi.nlm.nih.gov/sutils/splign/splign.cgi).

2.3. Developmental stage- and tissue-specific expression using quantitative real-time PCR

For developmental stage-specific analysis, the samples were prepared from the oocytes of female ovaries, the laid eggs from rice leaf sheaths, the first-fifth instar nymphs, the female and the male adults, individually. For tissue specificity, the fat body, gut, salivary gland, ovary, testis and integument were dissected from the fifth instar nymphs, female and male adults under a Leica S8AP0 stereomicroscope (Leica Microsystems GmbH, Wetzlar, Germany) and quickly washed in diethylpyrocarbonate-treated NaCl/Pi solution (pH 7.4) as previously described (Bao et al., 2014). Total RNA was extracted from each developmental stage and each tissue using a RNAiso plus kit (TaKaRa, Dalian, China). First-strand cDNA was synthesized using a Hiscript® II Q RT SuperMix for qPCR (+ gDNA wiper) Kit (Vazyme, Nanjing, China) to remove any contaminating genomic DNA. RNA with no-reverse-transcriptase was used as the no-template control. Quantitative real-time PCR (qPCR) was run on a CFX Connect™ Real-Time System (Bio-Rad, Hercules, CA, USA) using ChamQ™ SYBR® Color qPCR Master Mix (Vazyme, Nanjing, China) under the following reaction program: an initial denaturation step at 95 °C for 3 min followed by 40 cycles at 95 °C for 10 s and 60 °C for 30 s. The gene specific primers were designed using the Primer Premier 6.0 program based on the *N. lugens* transcriptomic sequences as shown in Supplementary file: Table S1. As the internal controls, expression of the *N. lugens* housekeeping gene for 18S ribosomal RNA, RPS11 and RPS15 (GenBank accession no. JN662398, XP_022188350 and ACN79501) was analyzed. The results were normalized to the expression level of the internal genes. The $\Delta\Delta C_t$ method _ENREF_26was used to evaluate the quantitative variation in

the transcript levels as described previously (Huang et al., 2016).

2.4. Preparation of antibody

Lugensin A coding region flanking by *Not* I/*Xoh* I sites was amplified using the following primers as shown in Table S1. The PCR product was cloned into pMD19-T plasmid (TaKaRa) to obtain a recombinant pMD19-T-*lugensin*-A vector. After *Not* I/*Xoh* I *digestion, the lugensin* A ORF was ligated into the pGEX-6P-1 expression vector with GST at the N terminus. Fusion protein GST-*lugensin* A was expressed in *E. coli* Rosstta under 1 mM of IPTG induction at 37 °C. The expressed protein bands were retrieved after SDS-PAGE and dissolved in phosphate-buffered saline (PBS). Rabbit immunization was performed and anti-GST-*lugensin* A serums were prepared as described by Huang et al. (2016). The polyclonal rabbit antibody against GST-*lugensin* A were used for immunoassay.

2.5. Western blotting assay

The 5th instar nymphs were injected with heat-killed *E. coli* K12, *B. subtilis* and *Aaa* RS-1. The naïve nymphs and the nymphs injected with sterilized PBS were used as the controls. The hemolymph was collected at 24 h after injection and the protein concentration was quantified using a Pierce BCA Protein Assay Kit (Thermo Scientific, Rockford, IL, USA) following the manufacturer's instructions. The 6 × protein loading buffer was added and boiled for 30 min. The proteins were separated by SDS-PAGE and transferred to PVDF membrane. The blot was probed with a lugensin rabbit primary antibody (1:100 dilution) and detected using a goat anti-rabbit IgG-conjugated horseradish peroxidase (HRP) antibody (HuaBio, Hangzhou, China) at a dilution of 1:5000. Western blot signals were developed using a Chemiluminescence Detection Kit (Bio-Rad, Hercules, CA, USA) and photographed with the Molecular Imager® ChemiDoc™ XRS + System (Bio-Rad, Hercules, CA, USA). The β-actin polyclonal rabbit serum was used to monitor equal protein loading. The Gray value of western blotting bands were analyzed by image J software (Sheffield, 2007).

2.6. LC-MS/MS

Hemolymph was collected as described above. The hemolymph proteins were separated by SDS-PAGE and stained with Coomassie Bright Blue. The protein bands of 10 KDa and 14 KDa were cut respectively out of the gel for LC-MS/MS analysis. The protein bands of 15 KDa were collected and used as a control. Each protein sample was added 100 mM NH_4HCO_3/30%ACN for decolorization until transparent, then was added with 100 mM NH_4HCO_3 and 100 mM DTT to incubate at 56°Cfor 30 min. The protein samples were alkylated with 200 mM IAA and digested with trypsin in 50 mM NH_4HCO_3 buffer overnight at 37 °C. LC − MS/MS analysis was performed as previously described (Cao et al., 2016; Huang et al., 2016). Briefly, the peptide mixture (20 μl) was loaded onto the trap column at a flow rate of 10 μl/min by Thermo Scientific Easy nanoLC 1000 (Thermo Fisher Scientific, MA, USA). After trap equilibration, the samples were eluted with a linear gradient of buffer A and B at a flow rate of 250 nl/min as described above. The chromatographic system includes a trapping column (75 μm × 2 cm, nanoviper, C18, 3 μM, 100 Å) and an analytical column (50 ìm × 15 cm, nanoviper, C18, 2 μM, 100 Å). Separated MS data were analyzed using Thermo LTQ-Orbitrap Velos Pro (Thermo Fisher Scientific, MA, USA) equipped Nanospray Flex ionization source and FTMS (Fourier transform ion cyclotron resonance mass analyzer) combined with Thermo LTQ-Orbitrap Elite equipped Ion Trap analyzer. The top 20 ions were chosen from a full mass scan (300–2000 m/z) by collision induced decomposition (1.0 m/z isolation width, 35% collision energy, 0.25 activation Q, 10 ms activation time). Dynamic exclusion duration was 60 s. Survey scans for MS1 were acquired at a resolution of 30,000 at m/z 400.

2.7. Construction of recombinant lugensin expression vector

The recombinant pMD19-T-*lugensin* A and pMD19-T-*lugensin* B vectors, as described *in 2.4 Preparation of antibody*, were digested with *Not* I/*Xoh* I enzymes, respectively. The released *lugensin* ORFs deleting the signal peptide sequences were ligated into the corresponding enzyme sites of multiple cloning site (MCS) of PET-28a to construct the recombinant expression vector PET-28a-*lugensin* A and PET-28a-*lugensin* B, respectively. Fusion proteins of Lugensin A and B with His-tag were expressed in *E. coli* Rosstta under 1 mM of IPTG induction at 37 °C. Recombinant Lugensin proteins were harvested from the supernatant and filtered by 0.22 μm Millipore filter membrane (Millipore, MA, USA). Each recombinant protein sample was ultrafiltered with a 30-kDa molecular-weight cutoff (MWCO) Amicon Ultra-15 Centrifugal Filter Device (Millipore, MA, USA) by centrifuging at 4000 × *g* for 1 h. The ultrafiltered recombinant protein samples with molecular weights lower than 30 kDa were obtained as previously described (Bao et al., 2011). The protein concentrations were quantified using the Pierce BCA Protein Assay Kit (Thermo Scientific, Rockford, IL, USA).

2.8. Inhibition activity assay

Antibacterial activity of Lugensins was determined by inhibition zone assay. Bacteria *Escherichia coli* K12 and *B. subtilis* strains were cultured in LB broth (pH 7.0) at 37 °C. The final concentrations of bacterial suspension were adjusted to optical density at 600 nm (OD_{600}) of 0.6 and 0.75, respectively. Rice bacteria *Aaa* strain RS-1 was cultured in LB broth (pH 7.4) at 30 °C. The final concentration of the bacterial suspension of *Aaa* was adjusted to OD_{600} of 0.6. Each 200 μl cell suspension (5×10^8 cells/ml) of the different bacterial strains was spread into agar plates (sterile Petri dishes of 10 cm diameter, Corning). Wells with a diameter of 6 mm were punched into the freshly poured agar plates and filled with 200 μl of 2-fold dilution series of the recombinant Lugensin A or B, starting at a concentration of 0.5 mg/ml in the well. The plates were incubated at 37 °C or 30 °C until bacterial growth was visible (18–48 h). The diameters of the growth inhibition zones were determined with a vernier caliper (SATA, Shanghai, China). To monitor the bacterial growth under Lugensin application, *E. coli* K12, *B. subtilis* and *Aaa* strains were cultured in LB broth (pH 7.4) to obtain OD_{600} of 0.15–0.2 as above described. Lugensin A and B was respectively added into each bacterial culture and the bacterial growth was determined by measuring OD_{600} using μQuant (Bio-Tek, Vermont, USA) at 1 h intervals for 24 h. Ampicillin was used as a positive control. Sterilized PBS and the PET-28a empty vector were used as negative controls.

2.9. Membrane permeability assay

Membrane permeability assay was performed according to the method (Farkas et al., 2017). Briefly, *E. coli* K12 or *B. subtilis* was cultured at 37 °C, and *Aaa* was cultured at 30 °C in Luria-Broth (LB) medium overnight. Each bacterial culture was diluted in fresh LB and grown until the cell density reached OD_{600} = 0.2. Each 200 μl bacterial cell suspension was centrifuged and collected. Bacterial cells were washed in sterile PBS solution (pH 7.4) twice and resuspended in 1 ml of PBS (3×10^7 cells/ml). Each 100 μl Lugensin A or B (2 mg/ml) was added in each bacterial culture at room temperature for 2 h. Untreated cells and treated ones with the proteins from PET-28a were used as negative controls; ampicillin (1 mg/ml) served as a positive control. After incubation, the bacterial cells were centrifuged at 5000 rpm for 10 min and resuspended in 100 μl of PBS. Then the cells were co-stained with two fluorescent nucleic acid dyes: SYTO-9 and propidium iodide (PI) of LIVE/DEAD® BacLight™ (Invitrogen, Carlsbad, CA, USA), and cultured in dark at 37 °C temperature for 15 min. SYTO-9 is a membrane-permeable nucleic acid dye that is able to stain all bacterial cells and shows green fluorescence; while PI is restricted to stain membrane-damaged cells (non-living cells) and shows red fluorescence (Boulos

Table 1
Identification of the most significantly differential expressed genes upon *PGRP-LC* knockdown and/or bacteria challenge.

Gene name	Best match	Similarity[a]	FC[b] (A/I)	FC (I/C)	FC (A/C)
unknown function gene	*Halyomorpha halys*	44%	6.39	−4.94	1.49
defensin	*Nilaparvata lugens*	100%	6.24	−4.58	1.69
PGRP-LC	*Nilaparvata lugens*	99%	3.72	−3.01	0.75

A: Activation. The 5th instar nymphs were injected with ds*GFP* followed by bacteria challenge.
I: Inhibition. The 5th instar nymphs were injected with ds*PGRP-LC* followed by bacteria challenge.
C: Control. The 5th instar nymphs were injected with ds*GFP*.
Bacteria: a mixed heat-killed *E. coli* K12 and *Bacillus subtilis* strains.
[a] similarity to the best match sequences.
[b] FC, fold change ($\log_2$ ratio) of gene expression.

et al., 1999). Live/dead bacterial cells were observed using a Zeiss LSM 800 confocal laser microscopy under 63 × magnification objective (Carl Zeiss MicroImaging, Göttingen, Germany). The excitation and emission wavelengths for SYTO-9 and PI were 488 nm/500 nm and 563 nm/617 nm, respectively.

2.10. Location of lugensin peptides in bacterial cells

Lugensins were labeled with FITC using the HOOK™ Dye Labeling Kit (Sangon, Shanghai, China) according to the manufacturer's instructions. *E. coli* K12, *B. subtilis* and *Aaa* RS-1 were respectively cultured in liquid LB medium at 37 °C or 30 °C until OD_{600} reached 0.1–0.2. Each 200 μl bacterial culture was resuspended in sterile PBS. FITC-labeling Lugensin A or B (2 mg/ml) was added in the bacterial culture and incubated at room temperature for 30 min, then co-stained with 800 nM FM4-64 membrane dye (Thermo, Waltham, USA). Fluorescence images were observed under a Zeiss LSM 800 confocal microscopy with 63 × oil objective (Carl Zeiss Micro Imaging, Gottingen, Germany). The excitation and emission wavelengths for FITC-labeling Lugensin A or B and FM4-64 membrane dye were 488 nm/500 nm and 563 nm/617 nm, respectively.

2.11. Scanning electron microscope (SEM)

E. coli K12, *B. subtilis* or *Aaa* were cultured in LB medium at 37 °C or 30 °C until OD_{600} reached 0.2–0.4 and resuspended in 1 ml of 0.1M PBS. Each 400 μg of the expressed proteins (pET28a-Lugensin A or B) was added in the bacterial culture and incubated for 4 h. Non-treatment and the expressed proteins (pET28a) were added as negative controls. Application with 200 μg of ampicillin served as a positive control. Bacteria was fixed in 2.5% (v/v) glutaraldehyde at 4 °C in 0.1M PBS (pH 7.4) overnight and washed in PBS three times. Post-fixation was performed with 1% (v/v) osmium tetroxide for 2 h at room temperature and washed in 0.1M PBS three times. The fixed bacterial cells were dehydrated through incubation in a graded series of ethanol (30, 50, 70, 80, 90, 95 and 100%, v/v) for 15 min each and then soaked in a mixed solution of ethanol and isoamyl acetate (v/v = 1:1) for 30 min. The samples were treated with isoamyl acetate overnight and dried in a desiccator under Leica EM CPD300 vacuum (Leica, Wetzlar, Germany). After gold-sputtering, the samples were observed under TM-1000 scanning electron microscope (Hitachi, Tokyo, Japan) at an acceleration voltage of 3 kV.

2.12. Phylogenetic analysis

The predicted *N. lugens* Lugensin A and B were aligned with the best matched orthologs of other insect species using the *ClustalW* program. The phylogenic trees were constructed by Maximum Likelihood using the program Mega 7.0 (http://www.megasoftware.net/). Phylogenetic relationships were determined using the bootstrap analysis with values of 1000 trials.

2.13. Availability of supporting data

The supporting data in this study have been submitted to the open access repositories. *N. lugens* genome assemblies have been deposited at GenBank under accession number AOSB00000000 (BioProject PRJNA177647). The *N. lugens* transcriptomic dataset is available in the Sequence Read Archive (SRA) database (http://www.ncbi.nlm.nih.gov/sra). The accession number of the *N. lugens* transcriptomic dataset is SRX023419. The transcript sequences of *N. lugens lugensin* genes were submitted to the National Center for Biotechnology Information (http://www.ncbi.nlm.nih.gov/). The genomic organization of exons and introns of the genes is predicted based on the mRNA-genome alignments by using GSDS 2.0 (Gene Structure Display Server) at http://gsds.cbi.pku.edu.cn/(Hu et al., 2014). The deduced protein domains and signal peptides were determined using Pfam (http://pfam.xfam.org/), SMART (http://smart.embl.de/) and InterProScan (http://www.ebi.ac.uk/Tools/pfa/iprscan/) as previously described. Molecular weight (Mw) and isoelectric point (pI) were analyzed using Compute pI/MW tool (http://web.expasy.org/compute_pi/).

3. Results

3.1. Identification of PGRP-LC regulated genes in N. lugens

To identify *PGRP-LC* regulated genes, we conducted RNA-Seq analysis by inhibiting *PGRP-LC* expression in *N. lugens* nymphs. A function-unknown gene and an antibacterial peptide *defensin* gene showed the most significant expression changes upon *PGRP-LC* knockdown and/or bacteria challenge. The expression of these two genes were increased approximately 1.5- and 1.7-fold, respectively, when challenged with a mixture of Gram-negative *E. coli* K12 and Gram-positive *B. subtilis* in ds*GFP*-treated nymphs (Table 1). Nevertheless, in ds*PGRP-LC*-treated nymphs, their expression was not up-regulated but rather down-regulated by bacterial challenge in comparison with ds*GFP*-treated controls (Table 1). The expression of the function-unknown and *defensin* genes were increased 6.4- and 6.2-fold, respectively, in the ds*GFP*-treated/bacteria-challenged nymphs when compared to the ds*PGRP-LC*-treated/bacteria-challenged nymphs. *PGRP-LC* gene expression was significantly decreased in the ds*PGRP-LC*-treated/bacteria-challenged nymphs in comparison with ds*GFP*-treated control, suggesting the effectiveness of the target dsRNA interference.

To obtain the complete sequence information of the function-unknown gene, we searched the *N. lugens* genomic and transcriptomic databases using its sequence as a query. Two cDNA sequences were identified at the transcriptional level. One is 922 base pair (bp) long that contains an open reading frame of 420 bp, a 263 bp of 5′ untranslated region and a 239 bp of 3′ untranslated region. The other sequence is 884 bp long that includes an open reading frame of 429 bp, a 212 bp of 5′ untranslated region and a 243 bp of 3′ untranslated region. The deduced peptides consists of 139 and 142 amino acid residues that share 74% sequence identity (Fig. 1A). The difference between the amino acid compositions was restricted to their N-terminal regions.

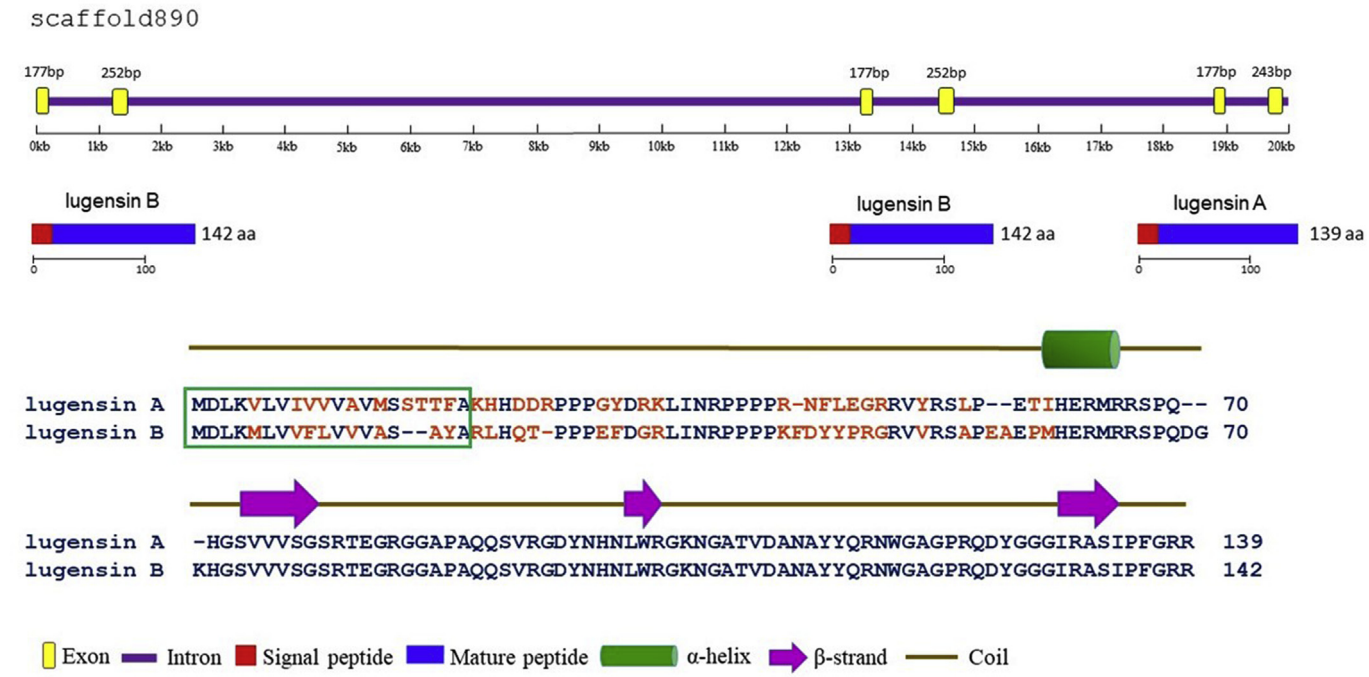

(A)

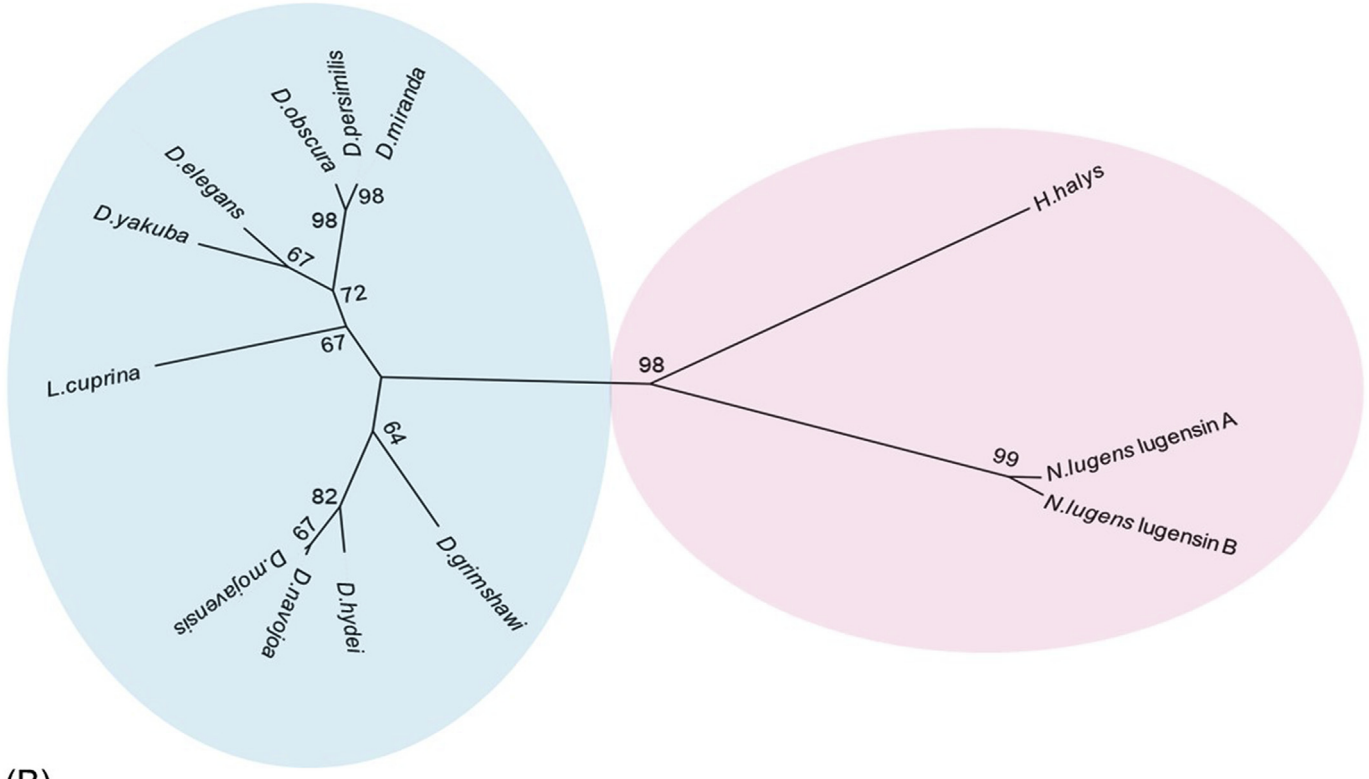

(B)

(caption on next page)

These two peptides were predicted to have the theoretical molecular mass of 15.58 and 15.81 kDa, and isoelectric points (*p*I) of 11.03 and 10.52, respectively, and are highly basic peptides. They had a putative signal peptide sequence of 20 and 18 amino acids, respectively, suggesting they are the secreted peptides. The amino acid sequences showed 44% and 35% similarities with a probable antibacterial peptide of *Halyomorpha halys* (GenBank accession no. XP_014273534). Here, we named the two genes as *lugensin* A (GenBank accession no. MH290357) and *lugensin* B (GenBank accession no. MH290358), respectively. Genomic-wide analysis revealed that *lugensin* A and B genes were located at a same scaffold and formed gene clusters (Fig. 1A). *Lugensin* A consists of two exons (177 bp and 243 bp). *Lugensin* B was repetitive

Fig. 1. Identification of *lugensin* genes in *Nilaparvata lugens*. (A) Location of *lugensin* genes on scaffold. The genomic organization of exons and introns of the genes is predicted based on the mRNA-genome alignments by using GSDS 2.0 (Gene Structure Display Server) at http://gsds.cbi.pku.edu.cn/(Hu et al., 2014). The exon regions are shown with yellow boxes. The putative signal peptides and mature peptides are marked by red and blue, respectively. Secondary structures of Lugensins were predicted by PSIPRED v3.3 (http://bioinf.cs.ucl.ac.uk/psipred/). Green and pink indicate α-helix and β-strand, respectively. Brown line is coil regions. The different amino acid residues between Lugensin A and B are shown in red. (B) Phylogenetic analysis of *N. lugens lugensin* genes. The phylogenetic tree was constructed by Maximum likelihood, using the program Mega 7.0 (http://www.megasoftware.net/). The Jones-Taylor-Thornton (JTT) for amino acid substitution model was used, the test of phylogeny was done by the bootstrap method with 1000 replications, bootstrap values > 50% are shown on each node of the tree. The GenBank accession numbers for the homologues sequences are as follows: *Drosophila persimilis* (XP_002026511.1), *Drosophila Miranda* (XP_017136772.1), *Drosophila hydei* (XP_023174179.1), *Drosophila yekuba* (XP_002095002.2), *Drosophila elegans* (XP_017111881.1), *Drosophila takahashii* (XP_017003507.1), *Drosophila navojoa* (XP_017955552.1), *Drosophila mojavensis* (XP_002008159.2), *Lucilia cuprina* (XP_023298006.1), *Drosophila grimshawi* (XP_001983979.1) and *Halyomorpha halys* (XP_014273534). (For interpretation of the references to color in this figure legend, the reader is referred to the Web version of this article.)

genes and each contains two exons (177 bp and 252 bp). Their predicted coding sequences of 420 bp and 429 bp in the genome were identical to the transcriptomic sequences. The fact that two or more *lugensin* loci are located at the same scaffold implied the gene duplications occurred in *N. lugens* genome. Amino acid composition showed that Lugensins are arginine-, proline- and glycine-rich peptides, which contain 18-19 arginine residues, 16–17 glycine residues and 12–14 proline residues with no cysteine residue. A tri-proline and a tetra-proline stretches present at the amino-terminus and a tri-glycine stretch present at the carboxy-terminus of the Lugensins. The structures of Lugensin A and B were predicted to have a α-helix of IHERMR/MHERMR, followed by three β-strands of SVVVSG, LWR and IRASI. The α-helixes and β-strands are connected by the flexible coil regions (Fig. 1A). The phylogenetic analysis revealed that two *N. lugens* Lugensins are related to a probable antibacterial peptide with unidentified function in *Halyomorpha halys*, which form an independent cluster and were distant from the uncharacterized proteins of several dipteran insects (Fig. 1B).

3.2. Tissue and development specificity of lugensin gene expression

We analyzed *lugensin* gene expression in different stages using qPCR. Similar to the expression profiles of *defensin* A and B, the *lugensin* A and B had the significantly highlevels in male adults and relatively low levels in female adults and nymphs (Fig. 2A). The *lugensin* transcripts were detected at low levels in the developing oocytes of female, but were not detectable in eggs laid in rice leaf sheaths (Fig. 2A). Tissue-specific analysis displayed that *lugensin* A and B transcripts were at very high levels in fat body, but low levels salivary gland, gut, ovary, testis and integument of the 5th instar nymphs, male and female adults (Fig. 2B). We compared *lugensin* expression with two *defensin* genes that are the only identified antibacterial peptide genes so far in *N. lugens*. *Defensin* A and B genes showed the similar development and tissue expression patterns with *lugensin* genes (Fig. 2A and B). Their transcripts had the highest levels in male adults in the developmental stages. Similarly, *defensin* transcripts were detected at significantly high levels in fat body of 5th instar nymphs and female/male adults. We also investigated the expression pattern of *PGRP-LC* gene, the key signal receptor in the Imd pathway. *PGRP-LC* transcript showed much higher levels in the male adults than the female adults and nymphs (Fig. 2A). *PGRP-LC* also expressed in the developing oocytes of female but almost did not express in eggs laid in rice leaf sheaths. This expression pattern is very similar between *lugensin* and *defensin* genes (Fig. 2A). Tissue-specificity showed that *PGRP-LC* had the highest transcript levels in gut, followed by fat body and integument of the 5th instar nymphs, male and female adults (Fig. 2B).

3.3. Expression regulation of lugensin genes

We investigated *lugensin* gene expression upon bacterial infection in the 5th instar nymphs. *E. coli* or *B. subtilis* injection significantly up-regulated *lugensin* expression at 24 h after bacterial challenge in nymphs (Fig. 3A). *Lugensin* A transcript levels increased 5.0- and 8.5-fold respectively in *E. coli*- and *B. subtilis*-injected nymphs when compared with non-infected (naïve) control; while *lugensin* B transcript levels increased 6.5- and 5.6-fold respectively in *E. coli*- and *B. subtilis*-injected nymphs. In ds*GFP*-treated nymphs, *lugensin* A transcript levels increased 4.9- and 8.4-fold respectively; whereas *lugensin* B transcript levels increased 9.19- and 4.7-fold respectively after *E. coli* or *B. subtilis* infection. The rice bacteria *Aaa* strain RS-1 challenge strikingly enhanced *lugensin* expression. *Lugensin* A and B transcript levels increased 242.4- and 21.7-fold respectively in *Aaa*-injected nymphs when compared with naïve control. In ds*GFP*-treated nymphs, *Aaa* infection increased *lugensin* A transcript levels to 143.2-fold; and increased *lugensin* B transcript levels to 21.7-fold. We compared *defensin* gene expression after bacterial infection. *Defensin* A and B genes showed the similar bacteria-triggered expression patterns. Their transcript levels were strongly activated by *E. coli*, *B. subtilis* and *Aaa* RS-1 (Fig. 3A). Among the tested bacteria, *Aaa* showed the strongest activity to induce *lugensin* and *defensin* gene expression.

To determine the signal pathway regulating *lugensin* and *defensin* gene expression, we aimed at a key receptor of the Imd pathway, *PGRP-LC* gene, which had the similar tissue and development specificity with *lugensin* and *defensin* genes, through the RNAi approach at *in vivo* level. It is notable that *E. coli* or *B. subtilis* injection did not increase the transcript levels of *lugensin* and *defensin* genes in ds*PGRP-LC* treated nymphs (Fig. 3A). *Aaa* RS-1 infection raised *lugensin* and *defensin* expression in ds*PGRP-LC* treated nymphs, but their transcript levels were much lower than those nymphs without ds*PGRP-LC* treatment. RNAi results indicate that *PGRP-LC* knock-down significantly inhibited or reduced bacteria-triggered *defensin* and *lugensin* gene expressions in *N. lugens* nymphs. qPCR analysis confirmed that the *PGRP-LC* transcript levels were greatly declined in ds*PGRP-LC* treated nymphs by approximately 92% and 90% when compared to no-treated (naïve) and ds*GFP*-injected controls in the 5th instar nymphs (Fig. 3B), indicating that RNAi sufficiently inhibited *PGRP-LC* expression.

3.4. Detection of the mature lugensin protein using LC-MS/MS

The theoretical molecular masses of Lugensin A and B without the signal peptide sequences were 13.5 and 13.9 kDa, respectively. Western blotting assay showed that the specific protein bands around 10 KDa and 14 KDa were detected in the hemolymph of the 5th instar nymphs that were injected with *E. coli* K12, *B. subtilis* or *Aaa* RS-1. Nevertheless, the protein bands of 10 KDa were not detectable in the hemolymph of the naïve and sterilized PBS-injected nymphs (Fig. 4A). The gray values of the protein bands of 10 KDa in the hemolymph of the bacteria-injected nymphs were significantly higher than that in the hemolymph of naïve and sterilized PBS-injected nymphs (Fig. 4A). LC-MS/MS showed that the peptide segments of GKNGATVDANAYYQR and SPQDGKHGSVVVSGSR of Lugensin sequences were detected in 10 KDa and 14 KDa protein bands, respectively (Fig. 4B), suggesting that 14 KDa proteins were the precursor proteins for Lugensins. The 10 KDa of peptides might be the mature Lugensin peptides that were excised from the precursor after enzymatic hydrolysis of the proteins. The amino acid sequences of Lugensin A and B contains the conserved motifs of RVYR and RVVR motifs, respectively (Fig. 4C). RxxR motifs were the cleavage site between prodomain and mature peptide region in many insect

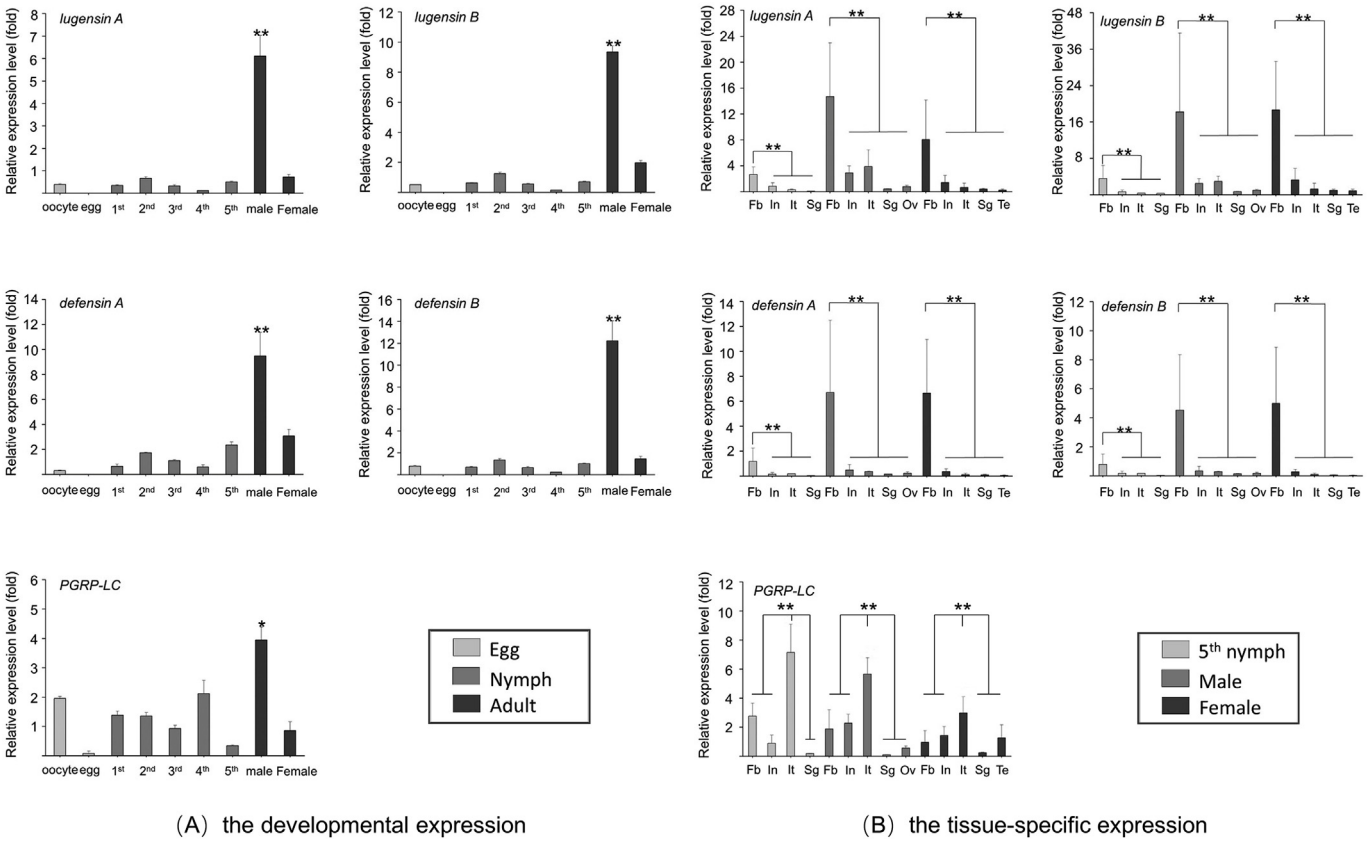

Fig. 2. Determination of gene expression patterns. (A) Developmental stage-specific expression (in fold) of target genes. Total RNA was extracted from the developing oocytes, laid eggs, nymphs and adults individually (n = 10–100; namely 100 oocytes or laid eggs; 20–80 nymphs and 10 adults) and used for expression analysis of target genes using qPCR. The relative expression levels of *lugensin*, *defensin* and *PGRP-LC* genes in each developmental stage or sex were normalized using *N. lugens RPS11*, *RPS15* and *18S rRNA* Ct values. Oocyte and laid egg refer to those from ovaries of female adults and from rice leaf sheaths, respectively. The 1st, 2nd, 3rd, 4th and 5th refer to the 1st–5th instar nymphs. *P* values are indicated (LSD-test). Asterisks (**) indicate significant difference ($p < 0.01$) from other developmental stages. (B) Tissue-specific expression (in fold) of target genes. Total RNA was extracted from the fat body (Fb), Intestine (It), salivary gland (Sg), ovary (Ov), testis (Te) and integument (In) of *N. lugens* nymphs, female and male adults (n = 20–80). First-strand cDNA was analyzed in each quantitative real-time PCR. Relative transcript levels of the target genes in the tested tissues were normalized using *N. lugens RPS11, RPS15, 18S rRNA* threshold cycle (Ct) values. Three biological replications (mean ± SD) were used, based on independent samples and the ΔΔCt method used to measure the relative transcript levels in each tissue. Results of triplicate experiments are shown with standard deviations. P values are indicated (Student's t-test). Asterisks (**) indicate significant difference ($p < 0.01$) from other tissues.

antibacterial peptides. We suppose that RVYR/RVVR motifs of Lugensins are the putative cleavage sites of the enzymatic hydrolysis.

3.5. Inhibition activity assay of the recombinant lugensin proteins

The recombinant Lugensin precursor proteins were obtained through prokaryotic expression and detected by western blotting assay. The sizes of recombinant Lugensin A and B were around 16 KDa as shown using 6 × his-tag and Lugensin A-specific rabbit primary antibody (Fig. 5A). In contrast, no specific protein band was detected in the protein samples expressed from an empty vector, which was used as a negative control. SDS-PAGE with CB staining showed the clear bands around 16 KDa in Lugensin A or B expressed products within the ranges of protein concentrations (0.5–2 mg/ml). No such a band was observed in the empty expression vector control. We determined the antibacterial activities of Lugensins using the plate growth-inhibition assay against different bacterial strains. The recombinant Lugensin A and B proteins showed antibacterial activities towards *E. coli* K12, *B. subtilis* and *Aaa* RS-1 (Fig. 5B). Apparent inhibition zones were observed after Lugensin application on each bacterial plate in the range of protein concentrations (0.5–2 mg/ml). Lugensins showed a dose-dependent antibacterial effect toward *E. coli* K12, *B. subtilis* and *Aaa* RS-1 (Fig. 5 B&C). Lugensin A had much potent activities against these bacteria than Lugensin B at each protein concentration (Fig. 5C). As a positive control, ampicillin had strong antibacterial activities against *E. coli* K12 and *B. subtilis*, but no activity towards *Aaa* RS-1. Application of sterilized PBS and empty vector PET-28a did not produce visible inhibition zone against *E. coli* K12, *B. subtilis* or *Aaa* RS-1.

Furthermore, we monitored the bacterial growth by measuring optical density at 600 nm under different applications for 24 h. In sterilized PBS or empty vector added cultures, the OD_{600} values of *E. coli* K12 gradually increased and reached 0.6–0.7; and the OD_{600} values of *B. subtilis* and *Aaa* RS-1 continually increased and reached 0.45–0.5 at 24 h (Fig. 5D). In contrast, in cultures added Lugensin A or B at concentration of 2 mg/ml, the OD_{600} values of *E. coli* K12 were only around 0.3 at the end of the test (24 h). The OD_{600} values of *B. subtilis* did not reach 0.3 throughout the test time period; while the OD_{600} values of *Aaa* RS-1 only reached 0.25 at 24 h of the culture. These observations indicate that addition of Lugensin A or B arrested the tested bacterial growth. As a positive control, ampicillin significantly inhibited *E. coli* K12 and *B. subtilis* growth as the OD_{600} values were consistently remained less than 0.1 within 24 h. However, ampicillin seemed not to affect the growth of *Aaa* RS-1 as shown by sustainably increased OD_{600} values. These results provide the further evidences showing that Lugensin A and B had antibacterial activities toward *E. coli*, *B. subtilis* and *Aaa* RS-1 strains. Moreover, Lugensin A had the stronger activity against these test bacterial strains than Lugensin B.

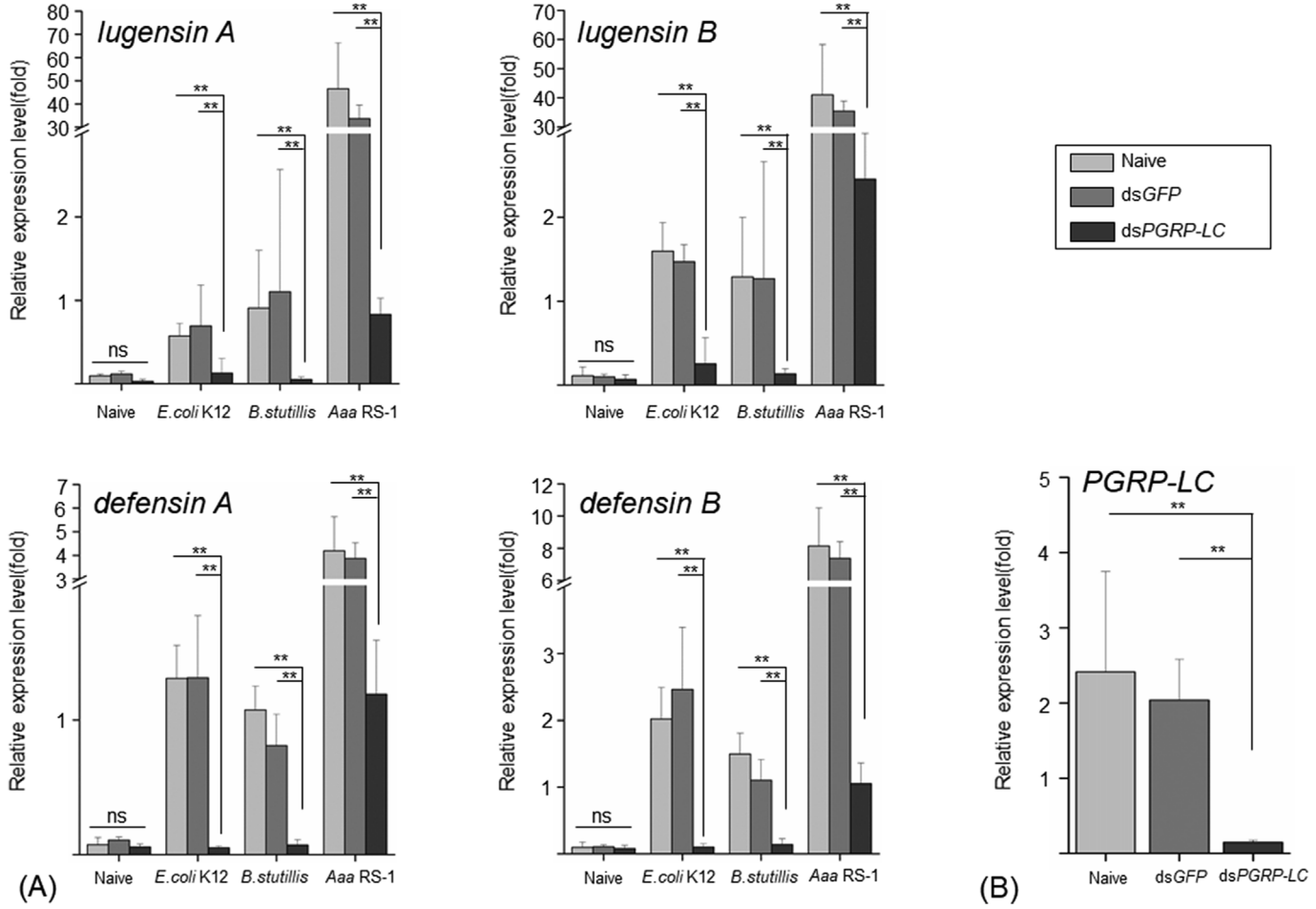

Fig. 3. Determination of the gene expression under PGRP-LC regulation in *N. lugens*. (A) *Lugensin* and *defensin* expression change upon *PGRP-LC* knockdown. The 3rd-instar nymphs were microinjected with ds*PGRP-LC*. The treated nymphs were reared at 26 ± 0.5 °C with 50 ± 5% humidity on fresh rice seedlings under a 16:8 h light: dark photoperiod for 24 h and then subjected to injection of *E. coli* K12, *B. subtilis* or *Aaa* RS-1 (5×10^7 cells/nymph). Total RNA was extracted from the nymphs at 24 h after bacterial injections. Two microlitres of first strand cDNA (10 ng) was analyzed in each quantitative real-time PCR reaction. PCR was performed with the specific primers for amplifying the target genes. The relative expression levels of each gene at different treatments were normalized using RPS11, RPS15 and 18S rRNA threshold cycle (Ct) values. In each assay, the expression level is shown relative to the lowest expression level, which is arbitrarily set to one. All samples were tested in three biological repeats. The means ± SD was used for analysis of relative transcript levels for each treatment using the $\Delta\Delta C_t$ method. Naive: Non-dsRNA treated control; ds*GFP*, ds*PGRP-LC*: ds*GFP* or ds*PGRP-LC* injected nymphs and then subjected to injection of *E. coli* K12, *B. subtilis* or *Aaa* RS-1 at 24 h p. i. (B) Effects of RNAi. *PGRP-LC* expression variation at 1 day post infection (d.p.i) in Non-dsRNA, ds*GFP* and ds*PGRP-LC* treated nymphs were determined by qPCR as previously described.

3.6. Effect of Lugensins on the membrane permeability of bacterial cells

SYTO-9 is a membrane-permeable nucleic acid dye that is able to stain all bacterial cells and shows green fluorescence; while PI is restricted to stain membrane-damaged cells (non-living cells) and shows red fluorescence. Treatment of *E. coli* K12 with Lugensin A produced red fluorescence, implying the damage of bacterial cell membranes and the cell death caused by Lugensin A application. When *E. coli* K12 was treated with Lugensin B, the bacterium displayed the visualized red and green fluorescence, suggesting the existence of membrane damaged cells (Fig. 6A). The results revealed that Lugensin A had the stronger activity than Lugensin B to induce the cell membrane permeability on *E. coli* K12 cells. Lugensin A or B treatment on *B. subtilis* and *Aaa* RS-1 generated red fluorescence, indicating that both of the proteins had strong antibacterial activities against *B. subtilis* and *Aaa* RS-1 (Fig. 6B and C). As negative controls, the untreated and the empty vector-treated bacterium displayed green fluorescence, implying the cell integrity of *E. coli* K12, *B. subtilis* and *Aaa* RS-1 strains (Fig. 6A–C). Treatment with ampicillin, which served as a positive control, led to the significant reduction or absence of green fluorescence in *E. coli* K12 and *B. subtilis* cells, confirming the strong bactericidal activities of ampicillin toward the bacteria (Fig. 6A and B). In contrast, only green fluorescence was observed in ampicillin-treated *Aaa* RS-1 cells, indicating no bactericidal effects of ampicillin on *Aaa* RS-1 strain (Fig. 6C).

3.7. Observation of scanning electron microscope (SEM)

SEM provides the ultrastructural evidence showing the damaging effects of Lugensins on the bacterial cells. Microscopic images captured the release of internal substances of *E. coli* K12 and *B. subtilis* cells after incubation with Lugensins for 4 h (Fig. 7). Leakage of cell content was clearly visualized around *E. coli* K12 and *B. subtilis* cells that were treated with Lugensin A or B; whereas no apparently cellular damage was observed in non- and empty vector-treated bacterial cells, suggesting that the *E. coli* K12 and *B. subtilis* cells were subjected to membranolytic destruction under lugensin treatment. SEM analysis showed the different effects of Lugensins on *Aaa* RS-1 strain. Treatment of *Aaa* RS-1 with Lugensin A or B for 4 h and 8 h did not produce apparent cell damage, but induced the pore formation and displays the leakage of cell content around the bacterial cells at 12 h. The pore formation and the leakage of cell content were not detected in the

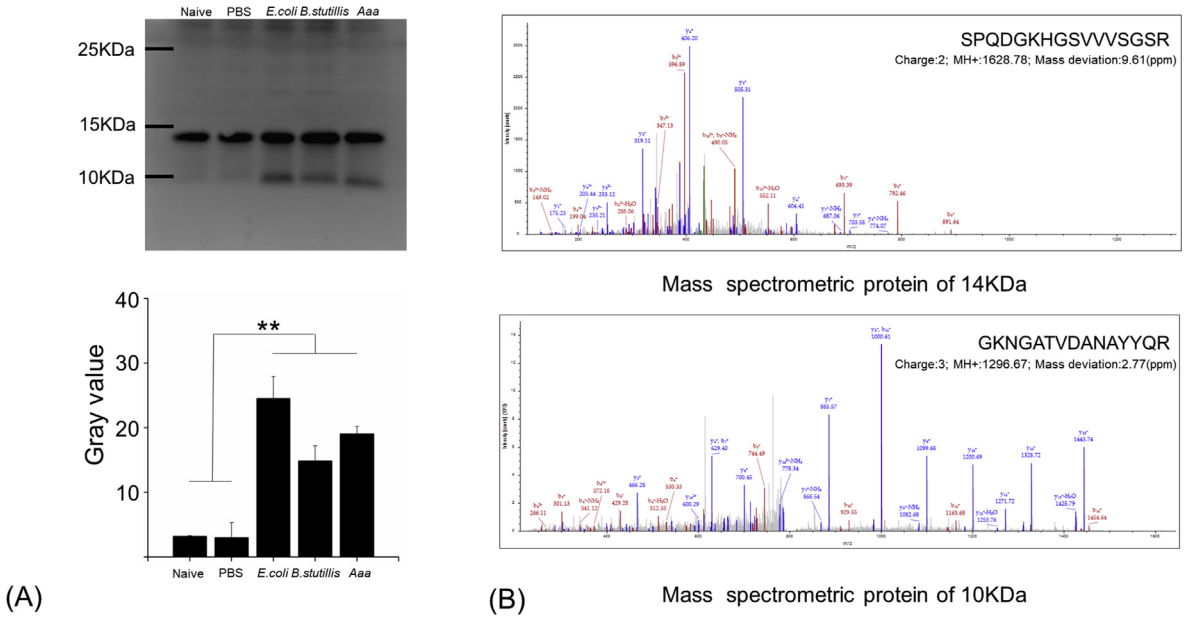


```
lugensin A   1 MDLKVLVIVVVAVMSSTTFAKHHDDRPPPGYDRKLINRPPPPRNFLEGRRVYRSLP--ETIHERMRRSPQ--- 71
lugensin B   1 MDLKMLVVFLVVVAS--AYARLHQTPPPEFDGRLINRPPPPKFDYYPRGRVVRSAPEAEPMHERMRRSPQDGK 71
               Signal peptide regions          the putative cleavage sites (RxxR)
lugensin A  72 HGSVVVSGSRTEGRGGAPAQQSVRGDYNHNLWRGKNGATVDANAYYQRNWGAGPRHDYGGGIRASIPFGRR 139
lugensin B  72 HGSVVVSGSRTEGRGGAPAQQSVRGDYNHNLWRGKNGATVDANAYYQRNWGAGPRQDYGGGIRASIPFGRR 142
```

Fig. 4. Detection of Lugensin proteins in hemolymph. (A) Detection of Lugensin proteins in the hemolymph of the 5th instar nymphs by western blotting assay. Gray value of the protein bands at 10 KDa and 14 KDa were analyzed by Image J software. Three biological replications were conducted. P values are indicated (Student's t-test). Asterisks (**) refers to the significant difference ($p < 0.01$). Naïve: naïve control; PBS: hemolymph collected from sterilization PBS-injected nymphs; *E. coli*, *B. subtilis*, *Aaa* refer to the hemolymph collected from *E. coli* K12, *B. subtilis* or *Aaa* RS-1 injected nymphs. (B) Annotated tandem mass spectra of the proteins of 10 KDa and 14 KDa, respectively. The precursor m/z, charge state and mass deviation are shown in each spectrum. (C) The putative cleavage sites of Lugensins for the enzymatic hydrolysis are marked in red. The mass-determined sequences were indicated in the amino acid sequence of full length Lugensin A and B are marked in brown and green, respectively. (For interpretation of the references to color in this figure legend, the reader is referred to the Web version of this article.)

control *Aaa* RS-1 cells, indicating that Lugensin applications led to the integrity change of *Aaa* RS-1 cell surface (Fig. 7). Ampicillin treatment resulted in complete membrane damage to *E. coli* K12 and *B. subtilis* strains, but did not change the membrane integrity of *Aaa* RS-1 strain. These results clearly suggest that Lugensins had the significant influence on the membrane integrity of bacterial cells.

3.8. Location of FITC-labeled lugensins in bacterial cells

To understand the action model of Lugensins on the tested bacteria strains, we investigated the location of FITC-labeled Lugensins in the bacterial cells after incubation for 0.5 h. The fluorescence of FITC-Lugensin A and B appeared in the *E. coli* K12 membranes but was hardly observed in the bacterial cytosol (Fig. 8A–D), suggesting that Lugensins act on the bacterial membrane of *E. coli* K12 strain. The accumulation of FITC-Lugensin A and B were clearly observed in the bacterial cytosol, but not in the membrane of *B. subtilis* cells, suggesting that the proteins might penetrate through the bacterial cell membrane and remained in the cytosol (Fig. 8). FITC-Lugensin A and B accumulated in both of the bacterial membrane and the cytosol of *Aaa* RS-1 cells (Fig. 8). These observations indicated that Lugensins had distinct action mechanisms on the different bacteria strains.

4. Discussion

Rice planthoppers have become the favorite hemipteran phloem-sucking insect species to study the interactions of insect-plant-virus, symbiotic relation, immune response and development mechanism due to the high efficiency of RNAi for functional characterization of genes. In our previous study, we identified a number of immune-related genes in the brown planthopper *N. lugens* by homology-based searches of the annotated genome coupled with transcriptomes (Bao et al., 2013). Different from that seen in some sap-sucking hemipteran insects, *A. pisum* and *B. tabaci*, the components for recognition and signaling to foreign microorganisms in the Toll, IMD, JNK and JAK/STAT pathways are conserved in *N. lugens*, suggesting the intact immune defense system in this insect species. *N. lugens* faces risks of encountering pathogens from natural rice crop environment, and therefore probably possesses a variety of immune responsive effectors to defense the pathogenic infection. Unexpectedly, only two classic antibacterial peptide genes, *defensin* A and B, were found in *N. lugens* so far. To investigate whether the non-classic antibacterial peptides exist in *N. lugens*, in the present study, we knocked down a key recognition receptor *PGRP-LC* in the IMD pathway and identified the differential expressed proteins between the *PGRP-LC* knockdown and control groups. Using RNA-seq combined with genome and transcriptome searching, we identified two function unknown genes named *lugensin* A and B, whose expression was strongly induced by bacteria-challenge, especially by a seed-borne rice pathogenic bacteria *Aaa* strain RS-1, but not in the *PGRP-LC*-knockdown planthoppers, indicating that the bacteria-induced *lugensin* gene expression was regulated via the PGRP-LC receptor. A NCBI searching failed to identify the significant sequence homologies of Lugensins with any characterized proteins. The only clue comes from a *H. halys* sequence encoding a probable antibacterial peptide that had low similarities (35–44%) with Lugensins. Based on this information, we determined to invest whether Lugensins have antibacterial activities. The

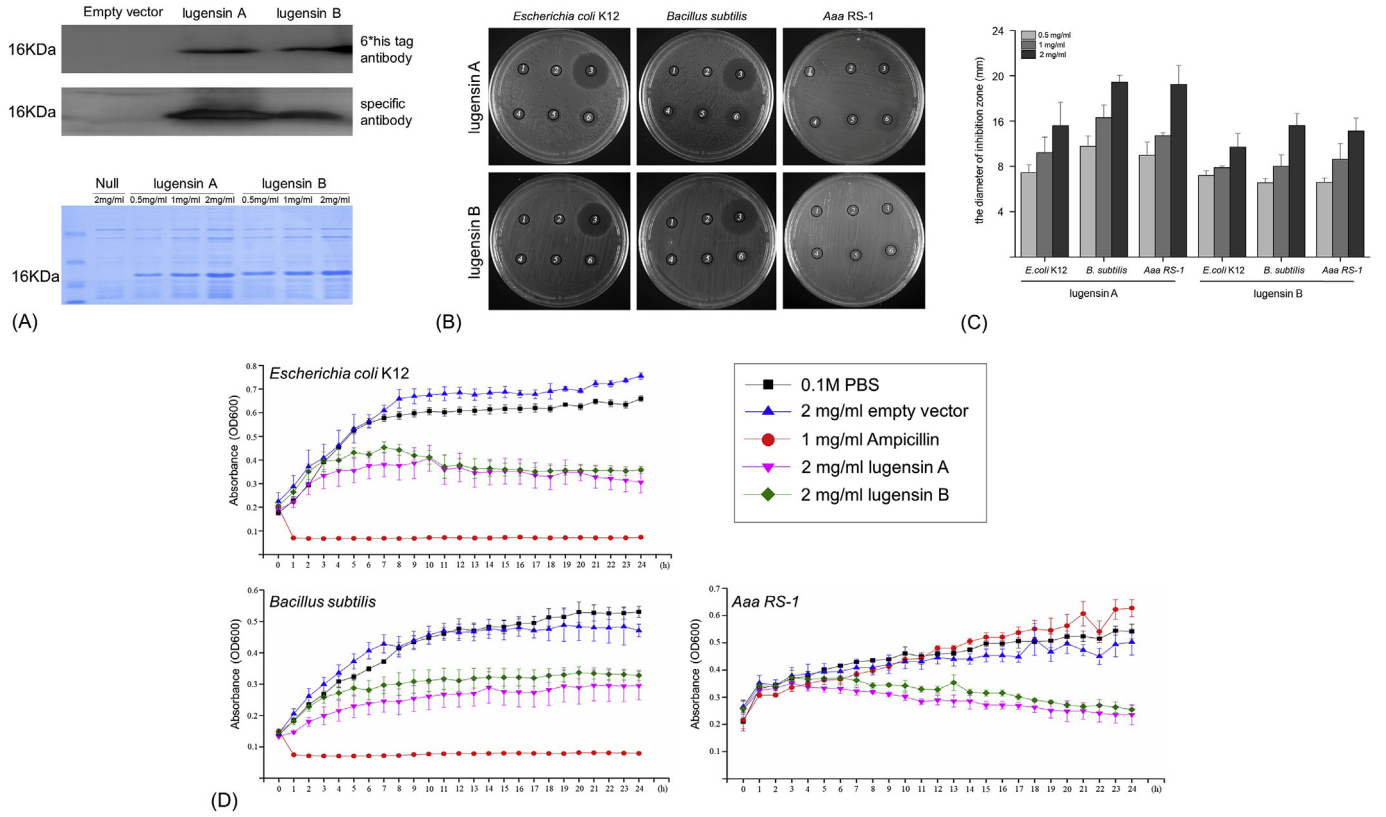

Fig. 5. Inhibition activity assay. (A) The recombinant Lugensin A and B proteins were analyzed using western blotting (the upper panel) and SDS-PAGE (the lower panel). The 6 × his tag rabbit antibody and Lugensin A-specific rabbit antibody were used to detect the specific protein bands, respectively. SDS-PAGE was stained with CB. The expressed proteins within the range of protein concentrations (0.5–2 mg/ml) were shown. The protein products from the PET-28a expression vector were used as a negative control. (B) The antibacterial effect of the recombinant Lugensin A and B against *E. coli* K12, *B. subtilis* and *Aaa* RS-1 was shown in each agar plate. 1 and 2 refer to sterile PBS and the protein products from PET-28a that were used as negative controls. 3 refers to Ampicillin at a concentration of 1 mg/ml that was used as a positive control. 4–6 refer to Lugensin A/B at a 2-fold dilution series (0.5 mg/ml, 1 mg/ml and 2 mg/ml). (C) Diameter of inhibition zones (millimeter) were defined using vernier caliper when a series dilution of Lugensin A and B were respectively applied to each bacteria-growth plate. (D) The antibacterial effect of the recombinant Lugensin A and B against *E. coli* K12, *B. subtilis* and *Aaa* RS-1 was measured the optical density at 600 nm under liquid culture conditions. The 2 mg/ml concentrations of Lugensin A and B were tested the antibacterial activity on bacterial growth. Ampicillin at a concentration of 1 mg/ml was used as the positive control. The protein products from PET-28a and sterile PBS were used as negative controls.

inhibition activity assay revealed that Lugensin A and B had apparent inhibitory activities against both Gram-negative and Gram-positive bacteria, suggesting that they are the antibacterial factors. The amino acid composition and the predicted structure showed that Lugensins are cationic but apparently do not resemble that of any known insect antibacterial peptide families, such as Cecropins, cysteine-rich Defensins (with three intramolecular disulfide bridges), proline-rich Drosocins/Lebocins, glycine-rich Attacins/Gloverins, proline- and glycine-rich Diptericins. Lugensins are rich in arginine, proline and glycine residues and have no cysteine residue. Many insect antibacterial peptides are predominantly expressed in fat body and hemocyte as precursor proteins with a “prosegement” and/or a “postsegment” sequences, and then the mature peptides are released into hemolymph. The mature antibacterial peptides are usually composed of 20–40 amino acid residues excised out from the preproproteins. We determined the molecular mass of Lugensins by western blotting analysis using Lugensin A antibody. The specific protein bands around 14 KDa were detected in the hemolymph of the 5th instar nymphs. The specific protein bands with 10 KDa were only observed in the bacteria-immunized hemolymph of the nymphs. Furthermore, LC-MS/MS confirmed that 10 KDa and 14 KDa protein bands contained the peptide segments of Lugensins. The theoretical molecular masses of Lugensin A and B deleting the signal peptide sequences were 13.5 and 13.9 kDa, respectively, suggesting that the 14 KDa protein bands might be the Lugensin precursors. As the protein bands of 10 KDa were present limited in the bacteria-immunized hemolymph, we speculate that the specific proteins likely to be the mature peptides that were released into the hemolymph after immune challenge.

Many insect antibacterial peptides are synthesized as the precursors, which generally have a conserved motif RxxR at the cleavage site between prodomain and mature peptide region (Shalini et al., 2018; Yang et al., 2018). The amino acid sequences of Lugensin A and B contain the conserved motifs of RVYR and RVVR motifs, respectively. We supposed that RVYR/RVVR motifs of Lugensins are most likely the cleavage sites of the enzymatic hydrolysis based on the predicted molecular masses of the putative mature Lugensin A and B with 9.41 KDa and 9.87 KDa. The Lugensin A and B precursor proteins are 139 and 142-amino acid long including signal peptides (20 and 18 amino acids), prosegments (29 amino acids) and mature peptides (90 and 95 amino acids). The Lugensin precursors are rich in proline/glycine residues and probably have some original functions other than delivering the mature peptides. In insects, the proline-rich and the glycine-rich antibacterial peptides are predominantly active on Gram-negative bacteria. Here, Lugensin precursors possess the apparent resistance to both Gram-negative and Gram-positive bacteria including *E. coli* K12, *B. subtilis* and the rice pathogenic bacteria *Aaa* RS-1. However, Lugensins did not show antibacterial activities toward the Gram-negative rice bacterial leaf blight pathogen *Xanthomonas oryzae* pv. *oryzae* (*Xoo*) strain and the rice blast fungal *Magnaporthe oryzae* (data not shown), suggesting that Lugensins had defense specificity toward the different rice pathogens.

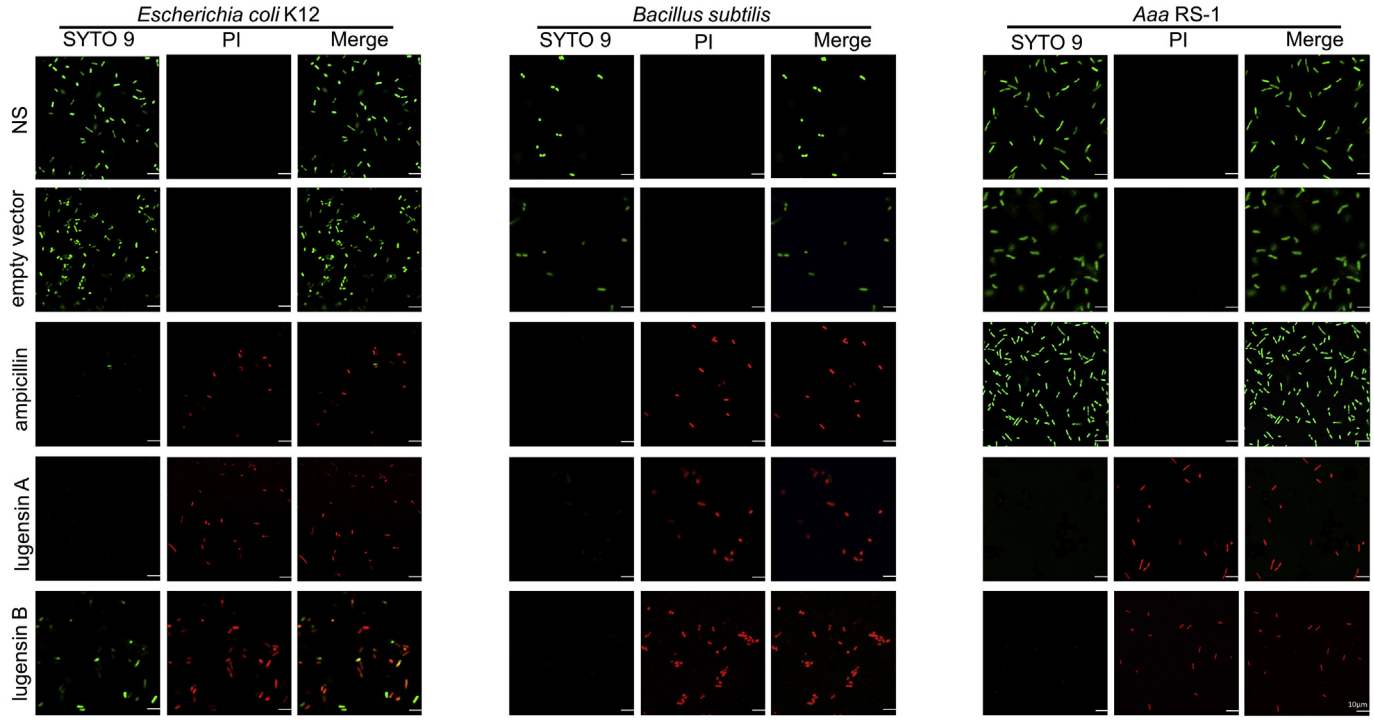

Fig. 6. Effect of Lugensins on bacterial membrane permeability. Fluorescence microscopy images of (A) *E. coli* K12 cells; (B) *B. subtilis* cells; (C) *Aaa* RS-1 cells treated with Lugensin A or B (2 mg/ml) for 4 h and stained with the fluorescent nucleic acid dyes of SYTO-9 and PI. Green fluorescence shows the integrate cell membrane (alive cells). Red fluorescence indicates the permeable membrane (non-living cells). Ampicillin treatment was used as positive control, non-treatment and the treatment with proteins from PET-28a empty vector were used as negative controls. Scale bar: 10 μm. (For interpretation of the references to color in this figure legend, the reader is referred to the Web version of this article.)

Most insect antibacterial peptides are cationic ones containing 2–8 positively charged amino acids, such as arginine and lysine. Cationic antibacterial peptides primarily act on electronegative bacterial cell surface and lead to cell lysis or disruption of bacterial membrane. Lugensin precursors contain more than 20 positively charged amino acids including 18–19 arginine residues and 3 lysine residues, suggesting the cationic property. The cationic properties enhance the affinity of Lugensins to bacterial cell surface. The α-helix structure in Lugensins helps the transient pore formation on the bacterial membranes and allows the antibacterial peptide enter the bacterial cells. The membrane permeability assay clearly displayed that Lugensin A or B damaged the integrity of the bacterial membranes of *E. coli* K12, *B.*

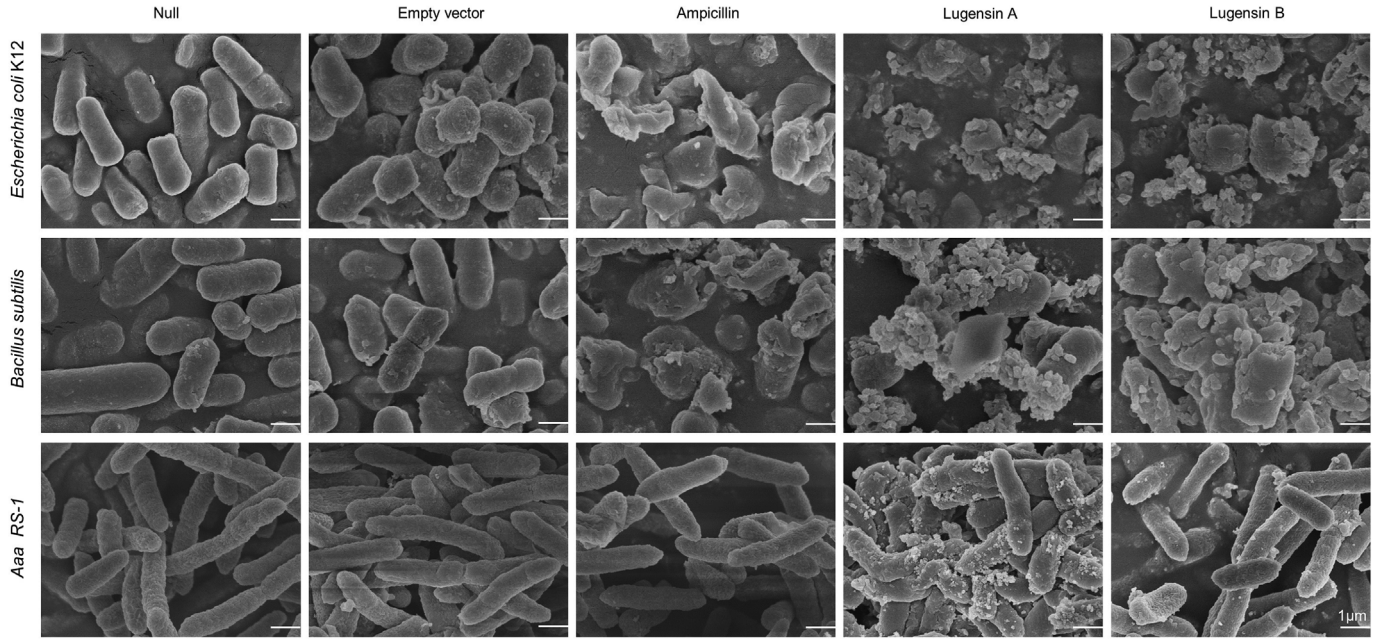

Fig. 7. Effect of Lugensins on bacterial cell integrity by scanning electron microscopy. *E. coli* K12 and *B. subtilis* strains were treated with Lugensin A or B (2 mg/ml) for 4 h; *Aaa* RS-1 strain was treated with Lugensin A or B for 12 h. Ampicillin treatment was used as positive control, non-treatment and the treatment with proteins from PET-28a empty vector were used as negative controls. Arrows indicate the leakage of internal substances around the bacterial cells. Scale bar: 1 μm.

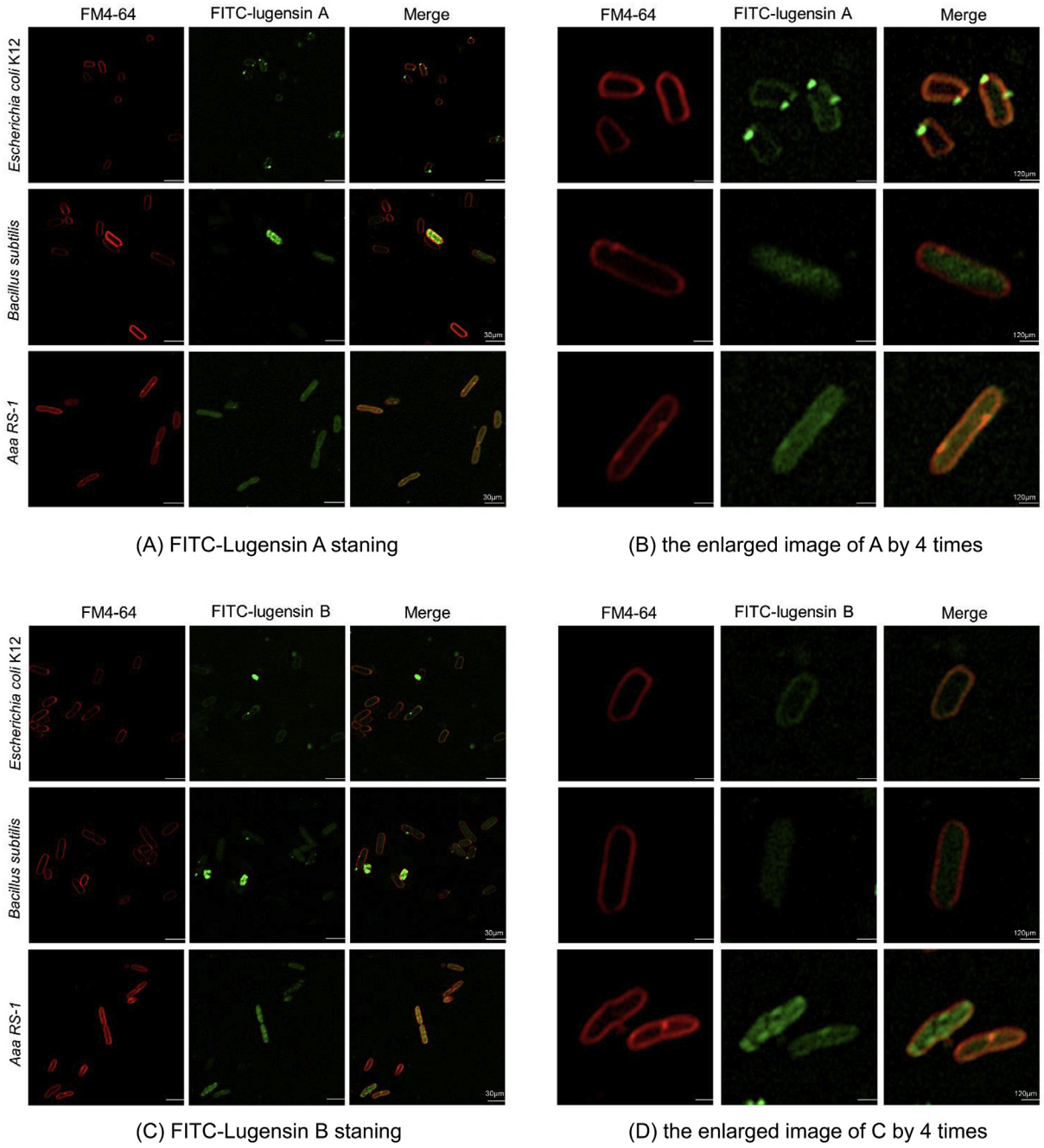

Fig. 8. Location of Lugensins in bacterial cells by immunofluorescence staining analysis. The tested bacterial strains were treated with FITC-labeled Lugensin A or B (2 mg/ml) and co-stained with FM4-64. (A) Greenish fluorescence signals indicate FITC-labeled Lugensins A; (B) the enlarged image of A by 4 times; (C) Greenish fluorescence signals indicate FITC-labeled Lugensins B; (D) the enlarged image of C by 4 times; Red fluorescence signals indicate FM4-64 labeled the bacterial membranes. Excitation and emission wavelengths were 488 nm and 500 nm for FITC, respectively; 563 nm and 617 nm for FM4-64, respectively. Scale bar: 30 μm and 120 μm. (For interpretation of the references to color in this figure legend, the reader is referred to the Web version of this article.)

subtilis and *Aaa* RS-1strains, which lead to cell death. Scanning electron microscopy provides the more direct evidence demonstrating the disruptive effects of Lugensins that caused the release of internal substances of *E. coli* K12 and *B. subtilis* cells. Differently, Lugensins did not cause the serious membrane damage of *Aaa* RS-1 strain, but affected the membrane integrity. Lugensins seemed to form pores on the *Aaa* RS-1 cell membrane and the internal substances of cells were released from the pores on the membrane, to a less extend compared to other two bacteria. To better understand the mode of action of Lugensins on bacteria, we investigated the protein localization in the bacterial cells by labelling the proteins with FITC. The observation indicated that Lugensins are located in the membrane of *E. coli* K12 but seemed not to accumulate in the cytosol. In contrast, Lugensins did not localize in the membrane but accumulated in the cytosol of *B. subtilis*. Different from *E. coli* K12 and *B. subtilis*, Lugensins retained in both of the membrane and the cytosol of *Aaa* RS-1. These observations suggested that Lugensins have the diverse membrane targets and/or intercellular targets on *E. coli* K12, *B. subtilis* and *Aaa* RS-1 strains. The interaction mechanisms of Lugensin and bacteria might be involved in the transmembrane pore-forming modes and/or the intracellular killing modes, *i.e.* inactivation of enzymes or inhibition of biomacromolecule synthesis including DNA, RNA, protein and lipid. Lugensin A showed more potent antibacterial activities than Lugensin B toward these bacterial strains. The reason might be due to the different amino acid composition at

their sequences. The Lugensins represents a very promising candidate for future *in vivo* work and may serve as a novel compound for developing antibacterial drug.

In conclusion, Lugensin A and B are quite different from the characterized antibacterial peptides in the aspects of amino acid composition, antibacterial specificity and action mode. These two novel antibacterial peptides are of the great potential for engineering bacterial disease resistance into rice crops to control plant diseases, such as the seed-born rice bacterial pathogens. In our next plan, we will determine the antimicrobial activity spectrum of Lugensin on more pathogenic microorganisms including bacteria, fungi and virus, and identify the target molecules of Lugensins on rice pathogenic microorganisms.

Author contributions

B.Y. conceived and designed the experiments and wrote the manuscript. B.Y. analyzed the *N. lugens* genome and transcriptome data. X.Z., L.P., Z.W., W.W., Z. Z., H.H. and L.C. performed experiments. Q. S. provided valuable suggestions and helped to revise the manuscript. All authors discussed the results and approved the final manuscript.

Notes

The authors declare that no competing financial interest.

Acknowledgements

We thank Prof. Bin Li (Department of Applied Bioscience of Zhejiang University) for kindly providing the rice bacterial brown stripe pathogen *Acidovorax avenae* subsp. *avenae* (Aaa) strain RS-1. This work was supported by the National Natural Science Foundation of China (Grant No. 31371934) and Pao Yu-Kong and Pao Zhao-long Scholarship for Chinese Students and Studying Abroad.

Appendix A. Supplementary data

Supplementary data to this article can be found online at https://doi.org/10.1016/j.ibmb.2019.103215.

References

Bao, Y.Y., Qin, X., Yu, B., Chen, L.B., Wang, Z.C., Zhang, C.X., 2014. Genomic insights into the serine protease gene family and expression profile analysis in the planthopper, *Nilaparvata lugens*. BMC Genomics 15, 507.

Bao, Y.Y., Qu, L.Y., Zhao, D., Chen, L.B., Jin, H.Y., Xu, L.M., Cheng, J.A., Zhang, C.X., 2013. The genome-and transcriptome-wide analysis of innate immunity in the brown planthopper, *Nilaparvata lugens*. BMC Genomics 14, 160.

Bao, Y.Y., Xue, J., Wu, W.J., Wang, Y., Lv, Z.Y., Zhang, C.X., 2011. An immune-induced reeler protein is involved in the *Bombyx mori* melanization cascade. Insect Biochem. Mol. Biol. 41, 696–706.

Boulos, L., Prevost, M., Barbeau, B., Coallier, J., Desjardins, R., 1999. LIVE/DEAD® BacLight™: application of a new rapid staining method for direct enumeration of viable and total bacteria in drinking water. J. Microbiol. Methods 37, 77–86.

Cao, J.Y., Xu, Y.P., Cai, X.Z., 2016. TMT-based quantitative proteomics analyses reveal novel defense mechanisms of *Brassica napus* against the devastating necrotrophic pathogen *Sclerotinia sclerotiorum*. J. Proteom. 143, 265–277.

Chen, W., Hasegawa, D.K., Kaur, N., Kliot, A., Pinheiro, P.V., Luan, J., Stensmyr, M.C., Zheng, Y., Liu, W., Sun, H., 2016. The draft genome of whitefly *Bemisia tabaci* MEAM1, a global crop pest, provides novel insights into virus transmission, host adaptation, and insecticide resistance. BMC Biol. 14, 110.

Christophides, G.K., Zdobnov, E., Barillas-Mury, C., Birney, E., Blandin, S., Blass, C., Brey, P.T., Collins, F.H., Danielli, A., Dimopoulos, G., 2002. Immunity-related genes and gene families in *Anopheles gambiae*. Science 298, 159–165.

Dziarski, R., 2004. Peptidoglycan recognition proteins (PGRPs). Mol. Immunol. 40, 877–886.

Evans, J., Aronstein, K., Chen, Y.P., Hetru, C., Imler, J.L., Jiang, H., Kanost, M., Thompson, G., Zou, Z., Hultmark, D., 2006. Immune pathways and defence mechanisms in honey bees *Apis mellifera*. Insect Mol. Biol. 15, 645–656.

Farkas, A., Maróti, G., Kereszt, A., Kondorosi, É., 2017. Comparative analysis of the bacterial membrane disruption effect of two natural plant antimicrobial peptides. Front. Microbiol. 8, 51.

Gerardo, N.M., Altincicek, B., Anselme, C., Atamian, H., Barribeau, S.M., De Vos, M., Duncan, E.J., Evans, J.D., Gabaldón, T., Ghanim, M., 2010. Immunity and other defenses in pea aphids, *Acyrthosiphon pisum*. Genome Biol. 11, R21.

Hetru, C., Hoffmann, J.A., 2009. NF-κB in the immune response of *Drosophila*. Cold Spring Harb. Perspect. Biol. 1 a000232.

Hu, B., Jin, J., Guo, A.Y., Zhang, H., Luo, J.C., Gao, G., 2014. GSDS 2.0: an upgraded gene feature visualization server. Bioinformatics 31, 1296–1297.

Huang, H.J., Bao, Y.Y., Lao, S.H., Huang, X.H., Ye, Y.Z., Wu, J.X., Xu, H.J., Zhou, X.P., Zhang, C.X., 2015. Rice ragged stunt virus-induced apoptosis affects virus transmission from its insect vector, the brown planthopper to the rice plant. Sci. Rep. 5, 11413.

Huang, H.J., Liu, C.W., Huang, X.H., Zhou, X., Zhuo, J.C., Zhang, C.X., Bao, Y.Y., 2016. Screening and functional analyses of *Nilaparvata lugens* salivary proteome. J. Proteome Res. 15, 1883–1896.

Hultmark, D., 2003. Drosophila immunity: paths and patterns. Curr. Opin. Immunol. 15, 12–19.

International Aphid Genomics Consortium, 2010. Genome sequence of the pea aphid Acyrthosiphon pisum. PLoS Biol. 8 e1000313.

Laughton, A.M., Garcia, J.R., Altincicek, B., Strand, M.R., Gerardo, N.M., 2011. Characterisation of immune responses in the pea aphid, *Acyrthosiphon pisum*. J. Insect Physiol. 57, 830–839.

Lemaitre, B., Hoffmann, J., 2007. The host defense of *Drosophila melanogaster*. Annu. Rev. Immunol. 25, 697–743.

Mahadav, A., Gerling, D., Gottlieb, Y., Czosnek, H., Ghanim, M., 2008. Parasitization by the wasp Eretmocerus mundus induces transcription of genes related to immune response and symbiotic bacteria proliferation in the whitefly *Bemisia tabaci*. BMC Genomics 9, 342.

Sackton, T.B., Lazzaro, B.P., Schlenke, T.A., Evans, J.D., Hultmark, D., Clark, A.G., 2007. Dynamic evolution of the innate immune system in *Drosophila*. Nat. Genet. 39, 1461.

Shalini, K., Arvind, K., Unni, A.P., Grace, T., 2018. Motif analysis of avian liver expressed antimicrobial peptide 2 (LEAP2). RJPT 11, 2496–2502.

Sheffield, J.B., 2007. ImageJ, a useful tool for biological image processing and analysis. Microsc. Microanal. 13, 200–201.

Tanaka, H., Yamakawa, M., 2011. Regulation of the innate immune responses in the silkworm, *Bombyx mori*. ISJ Invertebr. Surviv. J. 8, 59–69.

Wang, G., Li, X., Wang, Z., 2015. APD3: the antimicrobial peptide database as a tool for research and education. Nucleic Acids Res. 44, D1087–D1093.

Wang, Y., Fan, H.W., Huang, H.J., Xue, J., Wu, W.J., Bao, Y.Y., Xu, H.J., Zhu, Z.R., Cheng, J.A., Zhang, C.X., 2012. Chitin synthase 1 gene and its two alternative splicing variants from two sap-sucking insects, *Nilaparvata lugens* and *Laodelphax striatellus* (Hemiptera: Delphacidae). Insect Biochem. Mol. Biol. 42, 637–646.

Waterhouse, R.M., Kriventseva, E.V., Meister, S., Xi, Z., Alvarez, K.S., Bartholomay, L.C., Barillas-Mury, C., Bian, G., Blandin, S., Christensen, B.M., 2007. Evolutionary dynamics of immune-related genes and pathways in disease-vector mosquitoes. Science 316, 1738–1743.

Wu, W.J., Wang, Y., Huang, H.J., Bao, Y.Y., Zhang, C.X., 2012. Ecdysone receptor controls wing morphogenesis and melanization during rice planthopper metamorphosis. J. Insect Physiol. 58, 420–426.

Xi, Y., Pan, P.L., Ye, Y.X., Yu, B., Xu, H.J., Zhang, C.X., 2015a. Chitinase-like gene family in the brown planthopper, *Nilaparvata lugens*. Insect Mol. Biol. 24, 29–40.

Xi, Y., Pan, P.L., Ye, Y.X., Yu, B., Zhang, C.X., 2014. Chitin deacetylase family genes in the brown planthopper, *Nilaparvata lugens* (Hemiptera: Delphacidae). Insect Mol. Biol. 23, 695–705.

Xi, Y., Pan, P.L., Zhang, C.X., 2015b. The β-N-acetylhexosaminidase gene family in the brown planthopper, *Nilaparvata lugens*. Insect Mol. Biol. 24, 601–610.

Xu, H.J., Chen, T., Ma, X.F., Xue, J., Pan, P.L., Zhang, X.C., Cheng, J.A., Zhang, C.X., 2013. Genome-wide screening for components of small interfering RNA (siRNA) and micro-RNA (miRNA) pathways in the brown planthopper, *Nilaparvata lugens* (Hemiptera: Delphacidae). Insect Mol. Biol. 22, 635–647.

Xu, H.J., Xue, J., Lu, B., Zhang, X.C., Zhuo, J.C., He, S.F., Ma, X.F., Jiang, Y.Q., Fan, H.W., Xu, J.Y., 2015. Two insulin receptors determine alternative wing morphs in planthoppers. Nature 519 464.

Xu, L., Huang, H.J., Zhou, X., Liu, C.W., Bao, Y.Y., 2017. Pancreatic lipase-related protein 2 is essential for egg hatching in the brown planthopper, *Nilaparvata lugens*. Insect Mol. Biol. 26, 277–285.

Yang, L.L., Zhan, M.Y., Zhuo, Y.L., Pan, Y.M., Xu, Y., Zhou, X.H., Yang, P.J., Liu, H.L., Liang, Z.H., Huang, X.D., 2018. Antimicrobial activities of a proline-rich proprotein from *Spodoptera litura*. Dev. Comp. Immunol. 87, 137–146.

Yi, H.Y., Chowdhury, M., Huang, Y.D., Yu, X.Q., 2014. Insect antimicrobial peptides and their applications. Appl. Microbiol. Biotechnol. 98, 5807–5822.

Zhang, B.X., Huang, H.J., Yu, B., Lou, Y.H., Fan, H.W., Zhang, C.X., 2015. Bicaudal-C plays a vital role in oogenesis in *Nilaparvata lugens* (Hemiptera: Delphacidae). J. Insect Physiol. 79, 19–26.

Zhang, Y., Zhang, F., Li, B., Yang, Y., Ibrahim, M., Fang, Y., Qiu, W., Masum, M., Oliva, R., 2017. Characterization and functional analysis of clpB gene from *Acidovorax avenae* subsp. *avenae* RS-1. Plant Pathol. 66, 1369–1379.